

P R O C E E D I N G S



5th Latin American Congress on
Biorefineries
From laboratory to industrial practice
January 7-9, 2019 - Concepción, Chile



5th Latin American Congress on Biorefineries

From laboratory to industrial practice

January 7-9, 2019 - Concepción, Chile

ORGANIZED BY



SPONSORED BY



COLLABORATORS



MEDIA PARTNERS





Carbon aerogel-supported Ni for upgrading biomass-derived vapors: A Py-GC/MS approach

Luis E. Arteaga-Pérez^a, Oscar Gómez^b, Romel Jiménez^b, Romina Romero^c

^aChemical Engineering School, University of Bio-Bio. Avda. Collao 1202. Chile

^bCarbon and Catalysis Laboratory (CarboCat), Department of Chemical Engineering, University of Concepcion, Chile.

^cUnit for Technological Development, University of Concepcion, Chile.

Abstract

A comprehensive study of carbon aerogel-supported nickel (Ni/CAG) in the catalytic fast pyrolysis (CFP) of torrefied *Eucalyptus globulus* was performed in a micro-pyrolysis unit (Py-GCMS). Catalysts were characterized by N₂ adsorption-desorption at 77K, X-ray diffraction (XRD) and Transmission Electron Microscopy (TEM). Regardless the use of catalysts, the pyrolysis vapors produced from torrefied biomass were depleted in carboxylic acids (selectivity < 7%). Furthermore, the CFP decreased the selectivity to furans and ketones by almost 50%, while phenols increased in a similar proportion. Ni/CAG was active for hydrogenation under H₂-depleted atmosphere, presumably by a synergistic effect between water gas shift and reforming reactions with transalkylation and decarbonylation of phenolics and furanics. It was demonstrated that metal cluster sizes influenced the reaction routes by favoring hydrogenation on metal facets and deoxygenation on step/corners sites.

1. Introduction

Fast pyrolysis, is a non-selective and simple liquefaction technique that allows converting different feedstocks into gas, liquid (bio-oil) and solid (biochar) [1]. Specifically, bio-oil is considered a fuel or a feedstock for the separation/synthesis of more valuable products, including platform chemicals. Despite its demonstrated applications for heating (boilers and turbines) and blending with petroleum fractions, the high heterogeneity and poor fuel quality of crude bio-oil (i.e. high oxygen (>30 wt. %) and water contents (15 – 30 wt. %), acidity (2 < pH < 3), high viscosity (0.04 – 0.1 Pa·s)); impose the need for upgrading processes [1].

The integration of catalytic fast pyrolysis (CFP) and biomass pretreatments (demineralization, torrefaction, drying, etc.), is an effective way for controlling the composition of pyrolysis vapors to obtain upgraded bio-oils. In this sense, several authors have recently reported on the advantages of producing bio-oil by combining CFP with torrefaction [2,3]. Torrefaction is a mild pyrolysis process, as it occurs at relatively low temperatures (200–300 °C), in a non- or low- oxidizing atmosphere [4–6]. During such treatment, some O-containing groups are removed from individual polymers – mainly hemicellulose –, in the form of light volatiles such as acids and alcohols. The removal of carboxylic acids is of paramount importance for bio-oils stability, thus removing them during pretreatment, CFP or by *ex-situ* catalytic upgrading (e.g., ketonization) is highly desirable [7].

Therefore, in this study the effectiveness of CAG-supported Nickel for upgrading pyrolysis vapors from torrefied biomass is assessed. Particularly, the study is focused on the effect of Ni cluster sizes, reaction temperature and C-to-B ratio on the reaction routes for converting phenols and furans. The catalysts are analyzed by N₂ adsorption-desorption at 77 K, XRD,



compositional analysis and TEM. Finally, the possible reaction schemes are postulated on the basis of micro pyrolysis (py-GC/MS) analysis and equilibrium data.

2. Experimental

2.1 Torrefaction

Biomass samples (*Eucalyptus globulus*) were provided by a local producer as chips and were pretreated according to the procedures previously reported [8]. After that, biomass was torrefied considering the maximum devolatilization rate defined by Arteaga et al. [8]. Results of fdstocks characterization are presented below:

Table 2. Characterization of crude and torrefied *Eucalyptus globulus*.

Proximate wt.% (a.r)			Ultimate wt.% (d.a.f.)		
Proximate	Crude	Torr.	Element	Crude	Torr.
Moisture content	2.28	1.92	C	47.2	52.3
Volatile matter)	83.44	76.02	H	6.2	5.54
Fixed carbon	13.89	21.3	N	0.2	0.31
Ash	0.40	0.76	S	0.06	BDL
HHV (MJ/kg) _{d.b.} [9]	18.7	20.1	O*	46.34	41.85

*. Oxygen is calculated by difference from C,H,N,S

2.2 Catalysts preparation

Both catalysts were prepared at the same Ni loading (10 wt%_{d.b.}), via incipient wetness of nickel nitrate ((Ni(NO₃)₂ • 6H₂O, >99% purity, Merck) on carbon aerogel. After impregnation, the samples were dried at 105 °C for 4 h and ground again prior to reduction. The metal loading was corroborated by measuring the Ni content through inductively coupled plasma optical emission spectrometry (ICP-OES) using a PerkinElmer Optima 7000 DV ICP-OES series instrument. Reduction conditions were controlled to obtain different cluster sizes:

Cluster size 1 (D1): Reduction was performed in a fixed bed reactor under a constant flow of 40 mL/min H₂ using 2°C/min heating ramp from room temperature up to 400°C and keeping the sample at this temperature for 2h.

Cluster size 2 (D2): Reduction was performed in a fixed bed reactor under a constant flow of 40 mL/min H₂ by increasing the temperature up to 700°C at 5°C/min and holding the sample at 700°C for 2h.

2.3 Catalysts characterization

The catalysts were characterized by several techniques in order to obtain its structural, textural and morphologic properties. Main techniques were: X-ray diffraction (XRD), transmission electron microscopy (TEM) and N₂-adsorption. Mean cluster sizes were obtained from TEM measurements and compared to that calculated from Scherrer's equation (using XRD pattern).

2.4 Micropyrolysis (Py-GC/MS)

The Py-GC/MS experiments were carried out in a micropyrolysis system (EGA/PY-3030D, Frontier Laboratories) interfaced with a gas chromatograph (GC-2010 Plus, Shimadzu)



equipped with a single quadrupole mass spectrometry detector (QP 2010 Ultra, Shimadzu). The interface line was kept at 300°C in all the experiments and the pyrolysis products (1:50 split ratio) were separated in a BP10 capillary column (30 m x 0.25 mm) with 14% Cyanopropylphenyl polysiloxane as stationary phase. The GC thermal program was specified according to a procedure reported elsewhere [4] and, once separated, the pyrolysis products were analyzed in a MS detector (70 eV ionization) within a m/z range of 2-600. The identification of compounds in the py-GC/MS spectra was carried out by considering a minimum cut-off score of 80%, with respect to the National Institute of Standards and Technology (NIST) mass spectral database.

2.5 Data processing

Py-GC/MS cannot provide an accurately quantitative absolute analysis of the compounds formed during pyrolysis, because it does not allow collecting the reaction products. Nevertheless, a linear proportionality between the chromatographic peaks area corresponding to a particular compound and their concentration could be established. The area% count was normalized with respect to (100 – char wt.%):

$$char (wt. \%)_{a,b} = 100 \times \left[\frac{(M_{rem} - M_{cat})}{(M_{in/C} - t_o - B)} \right] \quad (1)$$

the following criteria were defined to discuss the effect of catalysts and operational parameters:

Selectivity of the i^{th} compound:

$$S_i = 100 \times \left(\frac{Peak Area_i}{\sum_{i=1}^n Peak Area_i} \right) \quad (2)$$

3. Results & Discussion

3.1 Catalyst characterization

3.2.1 Textural properties and structure

The catalyst support had an elemental composition typical of a carbon aerogel (C:92%, N:1.8%, H₂:0.6%, O₂:5.6%) [10,11].

Table 1. Textural and compositional data of catalysts

Catalysts	Mass fraction		Surface S _{BET} (m ² /g)	Pore diam. dP. (nm)	Pore volume VP. (cm ³ /g)	Cluster Sizes D _p (nm)
	wt. %					
	Mass balance*	ICP- OES				
CAG	-	-	520	14.0	0.21	-
Ni/CAG (D1)	10	9.5	464	11.2	0.19	9.8
Ni/CAG (D2)	10	9.6	452	11.3	0.21	21.8

*Theoretical concentration based on mass balance

The Ni loading on the support via impregnation and followed by treatment in pure H₂, did not significantly affect the textural properties of the support, as evidenced by the slight variations of S_{BET}, VP and dP. This allows inferring that after impregnation, the resulting clusters did not plug the pores. Furthermore, pore sizes are at least one order of magnitude higher than the kinetic diameter (σ) of the oxygenated compounds derived from biomass



pyrolysis ($0.4 < \sigma \text{ (nm)} < 0.8$) [12].

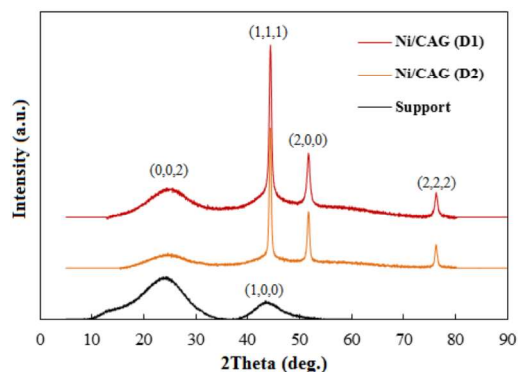


Figure 1. XRD patterns of catalysts and support

The XRD pattern of the support presents two broad reflections at 24° and 43° , which are commonly associated to the (002) and (100) graphitic planes in turbostratic carbons [13,14]. Similarly to previously reported by Arteaga-Pérez et al. [8], the signal at 24° was also visible in the catalyst's patterns. Both Ni/CAG (D1) and Ni/CAG (D2) exhibited three diffraction peaks at 44.5° , 51.7° and 76.45° , respectively. These peaks are typical of the (111), (200) and (222) planes in a face centered cubic structure (fcc) of Ni^0 and their presence indirectly demonstrate that the passivation avoided the bulk re-oxidation of metal particles [15]. The mean Ni^0 cluster size calculated by Scherrer's equation for Ni^0 in Ni/CAG (D1) was 11 nm, while for Ni/CAG (D2) it was almost double (20.7 nm).

3.2.2 Pyrolysis of torrefied *Eucalyptus*. Effect of catalysts

Pyrolysis vapor is a mixture of hundreds of organic species, thus analyzing the effect of operational parameters and/or catalyst properties—in the case of CFP—on product distribution is a challenge. Therefore, seeking for simplicity in the interpretation of py-GC/MS results, the compounds detected during py-GC/MS assays of torrefied biomass are first classified into eleven groups (Figs. 3a,b,c), following the IUPAC's naming rules for organic molecules [16]. All the experiments were replicated twice and the average standard deviations ranged between 8 and 11%.

When torrefied *Eucalyptus globulus* was subjected to CFP a significant change in product distribution was observed (Figs. 3a, 3b and 3c). The larger changes after CFP on Ni/CAG catalysts—regardless the Ni cluster sizes—, were observed for phenols (increased by ca.50%), furans (reduced by ca.50%), ketones (reduced by ca.50%) and gas (increased by 60%). Roughly, it could be inferred that the Ni^0 sites have promoted the upgrading of product vapors [17]. In the case of ketones, the selectivity reduction was due to decarbonylation, as can be inferred from the proportional increment in gas (mainly CO/CO_2) production.

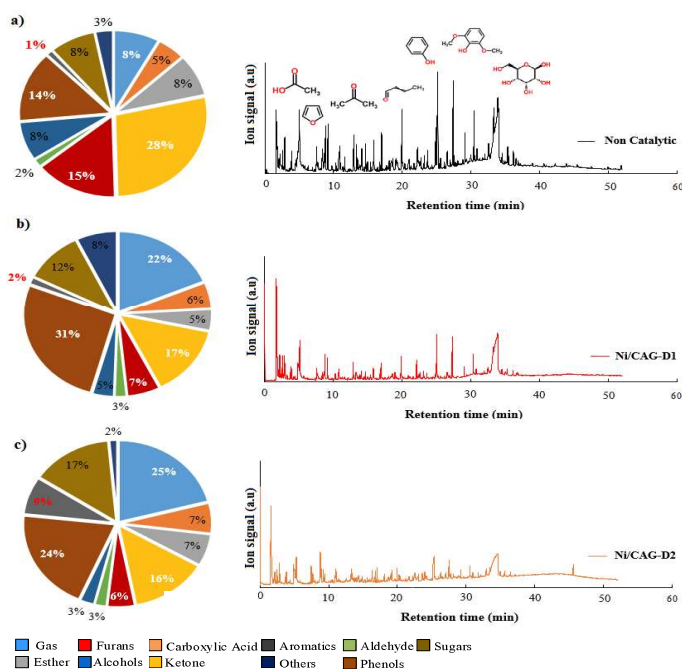


Figure 2. a) Non-catalytic pyrolysis b) Ni/CAG (D1) CFP, c) Ni/CAG (D2) CFP.
T=550°C. C-to-B= 10:1.

On the other hand, for phenols, there exist several alternative reaction routes (i.e. transalkylation, hydrogenolysis with subsequent C-O rupture, demethylation, etc.). A relatively accepted hypothesis is that *oxy*-compounds (i.e. phenols and furans) undergo direct deoxygenation or hydrogenation, which are strongly promoted by oxophilicity and hydrogenating sites (Ni^0). Despite some hypothetical conclusions, these *global* results do not allow interpreting the effect of catalyst properties nor operational parameters on the composition changes occurring within functional groups. However, a comprehensive analysis of these effects is mandatory to understand how the catalysts does interact with the biomass and biomass pyrolysis vapors to control the selectivity during a larger-scale process.

4. Conclusions

The catalytic fast pyrolysis of torrefied *Eucalyptus globulus*, over Ni/CAG favors the selectivity to more valuable fractions such as phenolics. While the production of furanics and ketones was reduced by 50% as compared with the regular pyrolysis (without catalysts). Furthermore, pyrolysis vapors from CFP were depleted in carboxylic acids, which allows inferring a better stability of corresponding bio-oils. Main changes in the composition of phenolics and furanics were correlated to Ni/CAG mean cluster sizes, temperature and C-to-B. Accordingly, the use of Ni/CAG (at 550°C and C-to-B>5:1) promoted the formation of furanics and phenols with a lower substitution degree, owing to the hydrogenating properties of Ni^0 sites.

5. Acknowledgments

This work has been financially supported by the project CONICYT-FONDECYT [grant



11150148, 2015], CONICYT-PCI [grant RED1170008, 2017] and Proyecto Basal [grant: Proyecto Basal AFB 170007].

6. Referencias

- [1] A. V. Bridgwater, Review of fast pyrolysis of biomass and product upgrading, *Biomass and Bioenergy*. 38 (2012) 68–94. doi:10.1016/j.biombioe.2011.01.048.
- [2] V. Srinivasan, S. Adhikari, S. Chattanathan, S. Park, Catalytic Pyrolysis of Torrefied Biomass for Hydrocarbons Production, *Energy & Fuels*. 26 (2012) 7347–7353.
- [3] A. Zheng, Z. Zhao, Z. Huang, K. Zhao, G. Wei, X. Wang, F. He, H. Li, Catalytic fast pyrolysis of biomass pretreated by torrefaction with varying severity, *Energy & Fuels*. 28 (2014) 5804–5811.
- [4] P. Basu, *Biomass Gasification, Pyrolysis and Torrefaction. Practical design and Theory*, 2nd ed., Elsevier Ltd, New York, 2013.
- [5] W.-H. Chen, J. Peng, X.T. Bi, A state-of-the-art review of biomass torrefaction, densification and applications, *Renew. Sustain. Energy Rev.* 44 (2015) 847–866.
- [6] A.L.M.T. Pighinelli, A. a. Boateng, C. a. Mullen, Y. Elkasabi, Evaluation of Brazilian biomasses as feedstocks for fuel production via fast pyrolysis, *Energy Sustain. Dev.* 21 (2014) 42–50. doi:10.1016/j.esd.2014.05.002.
- [7] A.M. Robinson, J.E. Hensley, J. Will Medlin, Bifunctional Catalysts for Upgrading of Biomass-Derived Oxygenates: A Review, *ACS Catal.* 6 (2016) 5026–5043.
- [8] L.E. Arteaga-Pérez, C. Segura, V. Bustamante-García, O. Gómez Cápiro, R. Jiménez, Torrefaction of wood and bark from *Eucalyptus globulus* and *Eucalyptus nitens*: Focus on volatile evolution vs feasible temperatures, *Energy*. 93 (2015) 1731–1741.
- [9] A. D5865-13, Standard Test Method for Gross Calorific Value of Coal and Coke., (2013).
- [10] M. Aegerter, N. Leventis, M. Koebel, *Aerogels handbook (Advances in Sol-Gel Derived Materials and Technologies)*, Springer, New York, 2011.
- [11] C. Moreno-Castilla, F.J. Maldonado-Hódar, Carbon aerogels for catalysis applications: An overview, *Carbon N. Y.* 43 (2005) 455–465.
- [12] J. Jae, G.A. Tompsett, A.J. Foster, K.D. Hammond, S.M. Auerbach, R.F. Lobo, G.W. Huber, Investigation into the shape selectivity of zeolite catalysts for biomass conversion, *J. Catal.* 279 (2011) 257–268.
- [13] Z.Q. Li, C.J. Lu, Z.P. Xia, Y. Zhou, Z. Luo, X-ray diffraction patterns of graphite and turbostratic carbon, *Carbon N. Y.* 45 (2007) 1686–1695.
- [14] L.E. Arteaga-Pérez, O. Gómez-Capiro, A. Delgado, S. Alejandro, R. Jiménez, Elucidating the role of ammonia-based salts on the preparation of cellulose-derived carbon aerogels, *Chem. Eng. Sci.* 161 (2017) 80–91.
- [15] R. Wojcieszak, M. Zieliński, S. Monteverdi, M.M. Bettahar, Study of nickel nanoparticles supported on activated carbon prepared by aqueous hydrazine reduction, *J. Colloid Interface Sci.* 299 (2006) 238–248. doi:10.1016/j.jcis.2006.01.067.
- [16] G. Yildiz, F. Ronsse, J. Verduyck, J. Daels, H.E. Toraman, K.M. Van Geem, G.B. Marin, R. Van Duren, W. Prins, In situ performance of various metal doped catalysts in micro-pyrolysis and continuous fast pyrolysis, *Fuel Process. Technol.* 144 (2016) 312–322.
- [17] N. Koike, S. Hosokai, A. Takagaki, S. Nishimura, R. Kikuchi, K. Ebitani, Y. Suzuki, S.T. Oyama, Upgrading of pyrolysis bio-oil using nickel phosphide catalysts, *J. Catal.* 333 (2016) 115–126. doi:10.1016/j.jcat.2015.10.022.